Evaluation of spherical fiducial localization in C-arm cone-beam CT using patient data

Ziv Yaniv[a)]
Department of Radiology, Imaging Science and Information Systems (ISIS) Center, Georgetown University Medical Center, Washington, DC 20007

(Received 16 March 2010; revised 8 July 2010; accepted for publication 13 July 2010; published 17 September 2010)

Purpose: C-arm based cone-beam CT (CBCT) has been recently introduced as an *in-situ* 3D soft tissue imaging modality. When combined with image-guided navigation, it provides a streamlined clinical workflow with, potentially, improved interventional accuracy. A key component in these systems is image to patient registration. The most common registration method relies on fiducial markers placed on the patient's skin. The fiducials are localized in the volumetric image and in the interventional environment. When using C-arm CBCT, the small spatial extent of the volumetric reconstruction makes this registration approach challenging, as the volume must include both the anatomy of interest and the fiducials. The authors have previously proposed a semiautomatic localization approach that addresses this challenge, with evaluation carried out using anthropomorphic phantoms. To truly evaluate the algorithm's utility, the evaluation must be carried out using clinical data. In this article, the authors extend the evaluation of the approach to data sets acquired in a clinical trial.

Methods: Nine CBCT data sets were obtained in three interventional radiology procedures as part of a clinical trial evaluating a commercial navigation system. Fiducials were localized in the volumetric coordinate system directly from the projection images using the evaluated localization approach. Localization was assessed using two quality measures fiducial registration error to quantify precision and fiducial localization error to quantify accuracy. The fiducials used in this study are 6 mm spheres embedded in a custom registration phantom used by the navigation system.

Results: In all cases, the proposed approach was able to localize all five fiducial markers embedded in the registration phantom. The approach's mean (std) fiducial registration error was 0.29 (0.13) mm. The mean (std) localization difference as compared to direct volumetric localization was 0.82 (0.34) mm.

Conclusions: Based on the current evaluation using data from clinical cases, the authors conclude that the localization approach is sufficiently accurate for use in thoracic-abdominal interventions, and that it can simplify the current workflow while reducing cumulative radiation to the patient due to repeated CBCT scans.
[DOI: 10.1118/1.3475941]

Key words: image-guided therapy, registration, fiducial localization, cone-beam CT, clinical evaluation

I. INTRODUCTION

Recent improvements in flat panel detector technology have led to improved tissue type discrimination, thus enabling the use of C-arm based cone-beam CT (CBCT) in clinical interventions dealing with soft tissue.[1–3] When combined with image-guided navigation, C-arm based CBCT provides a streamlined clinical workflow with, potentially, improved interventional accuracy.

A key component of image-guided navigation systems is registration, aligning image-space to patient-space. Once the transformation between the two coordinate systems is established, tracked instruments can be overlaid onto the image data, accurately reflecting the relationship between tools and anatomical structures in the physical world. The most common registration approach in clinical use is the analytic paired point rigid registration method.[4,5] When using C-arm based CBCT, the coordinates of corresponding points are obtained in the physical world, patient-space, and in the volumetric coordinate system of the CBCT, image-space.

One such navigation system that utilizes CBCT volumes and electromagnetic tracking for guiding thoracic-abdominal interventions is the iGuide CAPPA system (Siemens AG, Healthcare Sector, Erlangen, Germany). Figure 1 shows the system in use at Georgetown University Hospital. This system performs registration using a custom electromagnetically tracked phantom embedded with spherical fiducials that is imaged alongside the patient. The spherical fiducials are automatically localized in the reconstructed volume, automating the image to patient registration task. Note that for accurate guidance of thoracic-abdominal interventions, the use of rigid registration requires that images be acquired at breath hold and that the physician's actions be limited to the respiratory phase in which the images were acquired.

A key requirement of this registration approach is that

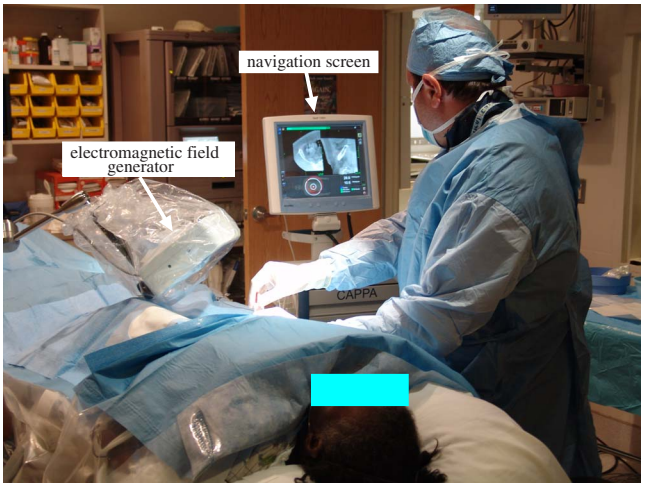

FIG. 1. Clinical case using the iGuide CAPPA navigation system. The system utilizes electromagnetic tracking and CBCT data to provide navigation guidance.

both the anatomical structure of interest and the fiducials placed on the patient's skin be inside the reconstructed region. This is a challenging requirement when using a C-arm based CBCT system, due to the small size of the spatial reconstruction region. Figure 2 illustrates this issue. This has also been identified as a limitation for hepatic interventional radiology procedures where a complete volume of the liver, often, could not be acquired.[2] In the context of image-guided navigation, we have previously identified this challenge and proposed a solution that enables localization of spherical fiducials outside the reconstructed region.[6] The proposed localization approach was evaluated using two types of anthropomorphic phantoms and two types of spherical fiducials.

On the one hand, these phantom studies enabled us to conduct a comprehensive evaluation of our algorithm in a controlled manner. On the other hand, they are only an approximation of clinical input. Most often, clinical data are more challenging. In our case, the clinical images contain additional medical apparatus that was not present in our phantom studies.

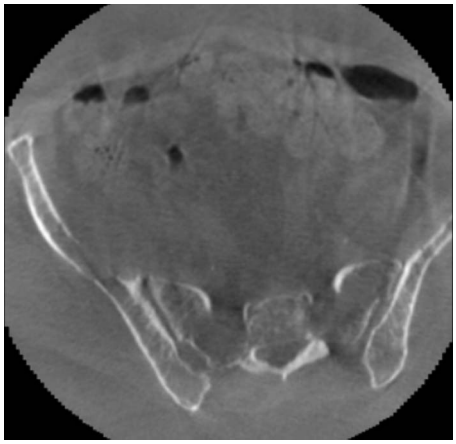

FIG. 2. Axial slice from an abscess drainage case. Data were acquired with the Siemens Axiom Artis dFA C-arm CBCT system. Reconstruction extent does not encompass the patient's body.

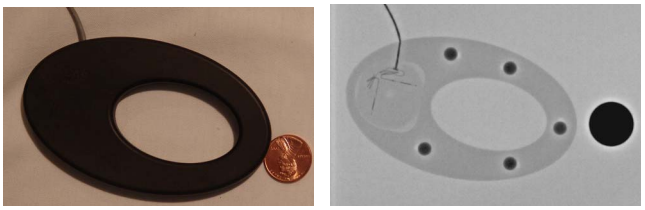

FIG. 3. Picture and x ray of the iGuide CAPPA registration phantom used in this work.

In this work we evaluate our approach using data acquired in a clinical trial utilizing a commercial navigation system in conjunction with C-arm based CBCT. We show that acquiring a reconstruction that contains both the fiducials, placed on the patient's skin, and the anatomical region of interest is indeed a challenging task. We also show that our fiducial localization approach can mitigate this limitation of the C-arm based CBCT reconstruction, potentially reducing both the procedure complexity and the radiation exposure to the patient.

II. MATERIALS AND METHODS

To evaluate the utility of a commercial navigation system in interventional radiology procedures the iGuide CAPPA system was used in an Institutional Review Board (IRB) approved clinical trial at Georgetown university hospital. All data used in the current evaluation was obtained as part of that trial which consisted of three navigated abscess drainage cases.

II.A. Equipment and image acquisition

All images used in this work were acquired with the Axiom Artis dFA (Siemens AG, Healthcare Sector, Erlangen, Germany) CBCT system. The CBCT is modeled as a distortionless pinhole camera. Projection images are acquired using an 8 s rotation, in which 419 images are uniformly acquired over a rotation of 209°. Image dimensions are 480×616 pixels with an isotropic pixel spacing of 0.61 mm. The size of the volumetric reconstructions obtained from these projection images is $256 \times 256 \times 221$ with an isotropic 0.8 mm voxel dimension, resulting in a reconstruction region with a spatial extent of approximately $20 \times 20 \times 18$ cm^3.

This acquisition protocol is intended for use in abdominal interventions and is a compromise between the length of a breath hold and the number of acquired images. In all cases, patients were requested to hold their breath during the acquisition.

The fiducial markers used in this work are 6 mm markers embedded in the custom iGuide CAPPA registration phantom. This phantom consists of five fiducials in a rigid configuration. Figure 3 shows the registration phantom and the internal fiducials.

TABLE I. Fiducial localization in volumetric coordinate system.

Initial 2D Localization in Single Projection Image
a. Manually define a rectangular ROI.
b. Perform edge detection in the ROI and fit a circle to the edge data using the RANSAC algorithm.
⇩
Initial 3D Localization (adjacent projection images, ±10° C-arm rotation)
a. Perform edge detection in a ROI defined by the epipolar line corresponding to the fiducial location estimated in the previous phase and fit a circle to the edge data using the RANSAC algorithm.
b. Compute the back–projected ray emanating from the x–ray source and going through the fiducial's 2D location.
c. Estimate the intersection point of the rays using the RANSAC algorithm.
⇩
Final 3D Localization (every n'th, n=10, image)
a. Project the initial 3D location onto the images.
b. Perform edge detection in a ROI centered on the projected point and and fit a circle to the edge data using the RANSAC algorithm.
c. Compute the back–projected ray emanating from the x–ray source and going through the fiducial's 2D location.
d. Estimate the intersection point of the rays using the RANSAC algorithm.

II.B. Localization approach

In the interest of making this presentation self-contained, we briefly describe our localization approach. We have observed that most often, fiducials that are outside the reconstructed region are visible in multiple projection images. We thus localize fiducials in the CBCT coordinate system by localizing them in the projection images. The spatial location of each of the fiducials is then estimated as the intersection point of the backprojected rays emanating from the camera locations and going through the corresponding image locations. Both the 2D fiducial location in the projection images and the ray intersections are estimated in a robust manner using the random sample consensus (RANSAC) algorithm.[7] This enables us to deal with outlying edge elements used in the circle detection process and with erroneous circle estimates used in the spatial localization.

Table I summarizes our fiducial localization approach. For further details, see Ref. 6.

II.C. Localization quality measures

To evaluate our localization approach, we use two quality measures: precision and accuracy. The former quantity is assessed independently for direct localization and for our approach. The latter assumes that direct localization is the gold standard and compares our approach to it.

For all data sets, we compute the fiducial registration error[8] (FRE) $\mathrm{FRE}=\sqrt{\frac{1}{N}\Sigma_{i=1}^{N}\|q_i-T(p_i)\|^2}$, where q_i and p_i are the paired points and T is the estimated rigid transformation. We can compute the FRE, as the fiducials are in a known fixed configuration inside the registration phantom. While this measure is uncorrelated with the target registration error,[9] it does assess the rigidity of the localized fiducial configuration. That is, given that we localize each fiducial on its own, the FRE quantifies the precision of the approach. If an approach has a bias, FRE will not reflect this as the rigid registration will compensate for this error component.

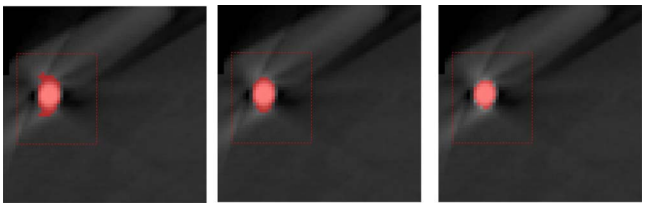

FIG. 4. Effect of threshold value on visually detectable fiducial segmentation. Segmentation overlaid onto original image. From left to right, oversegmentation 1800 HU, valid segmentation 2000 HU, and undersegmentation 2800 HU.

To asses our algorithm's accuracy, we use an additional quality measure for a subset of the data. For the data sets in which fiducials are inside the reconstructed region, we compare our results with direct fiducial localization in the volumetric data. While the true location of the fiducials remains unknown, direct fiducial localization is the standard localization approach used in clinical practice. Previously,[6] we used an edged based method for direct fiducial localization. The results of that method for the current data sets were found to be inaccurate, based on visual inspection. These inaccuracies stem from a significant reduction in the number of edge elements belonging to the fiducial surface. In previous studies, the volumes were reconstructed with an isotropic voxel dimension of 0.4 mm vs the current reconstructions which have an isotropic voxel dimension of 0.8 mm. As a result, the number of surface elements $s=4\pi r^2$ in the patient data sets is approximately a quarter of the elements available in the previous reconstructions.

We now use an intensity based method for direct localization. Fiducials are segmented using an empirically selected threshold, with the fiducial location estimated as the intensity weighted centroid of the segmented marker. The specific threshold value used for segmentation was determined visually. In our case, this value is set to 2000 HU. The effect of threshold selection on fiducial location was evaluated by varying the threshold until oversegmentation or undersegmentation was visually discernable. In our case, these occurred at 1800 and 2800 HU, respectively. The fiducials were then localized with threshold values between 2000 and 2600 HU. The maximal difference in between these localizations was 0.14 mm, a stable localization when using thresholds whose effects could not be visually detected. Figure 4 illustrates the visual effect of threshold value selection.

III. EXPERIMENTAL EVALUATION

The localization approach described above was implemented in MATLAB (The Mathworks Inc., Natick, MA). All evaluations were performed using a PC, Intel Core2 Duo 2.2 GHz processor, 4 GB RAM, running Windows Vista business edition.

Image data were acquired in three navigated abscess drainage cases. In total, nine scans were acquired in order to fulfill the requirement that both the anatomy of interest and the registration phantom be inside the reconstructed region. It should be noted that the navigation system requires that all five fiducials embedded in the registration phantom be localized in the volumetric reconstruction even though three fiducials are sufficient for rigid registration. Most likely, this is due to safety and accuracy considerations. As a result of these restrictions, additional CBCT images were acquired either due to fiducials that were outside the reconstructed region or, in one case, the targeted region was partially outside the volume.

TABLE II. Fiducial localization results. Columns denote the number of fiducials that could be localized directly in the volumetric reconstruction or, using the projection images, our approach. In all cases, our approach successfully localized the five fiducials comprising the registration phantom.

Data set		Fiducials from reconstruction	Fiducials from projection images
Patient 1	1	0	5
	2	4	5
	3	5	5
Patient 2	1	0	5
	2	4	5
	3	5	5
	4	5	5
Patient 3	1	0	5
	2	5	5

The mean (std) running time of our localization approach was 1.99 (0.24) s per fiducial. This is approximately half the running time observed with our previous data sets. The shorter runtime is consistent with the reduced data size; the size of the projection images used in the current study is half of that used in our previous work.

III.A. Qualitative evaluation

In all acquisitions, our approach was able to successfully localize the five fiducials, whether they were inside or outside of the reconstructed region. Table II summarizes the fiducial localization results both for our approach and for direct localization, the current clinical standard. Had our approach been used in these cases, the radiation dose to the first patient would have been a third of the actual dose, to the second patient it would have been a quarter, and to the third patient it would have been one half of the dose.

These results illustrate the difficulty of acquiring images so that the reconstructed region includes both the organ of interest and the fiducials on the skin surface. While initial positioning prior to the scan involves acquisition of anterior-posterior (AP) and lateral projection images, this does not ensure the desired results. In all three cases, the registration phantom was initially outside the reconstructed region even though it was visible in the AP and the peripheral region of the lateral image. This is primarily due to the practice of positioning the patient so that the organ of interest is close to the center of the reconstructed region and then ensuring that the phantom is still visible. Finally, if the emphasis shifts to ensuring that the phantom is in the reconstructed region, the organ of interest may be partially or completely outside the volume, resulting in an additional scan. This was the situa-

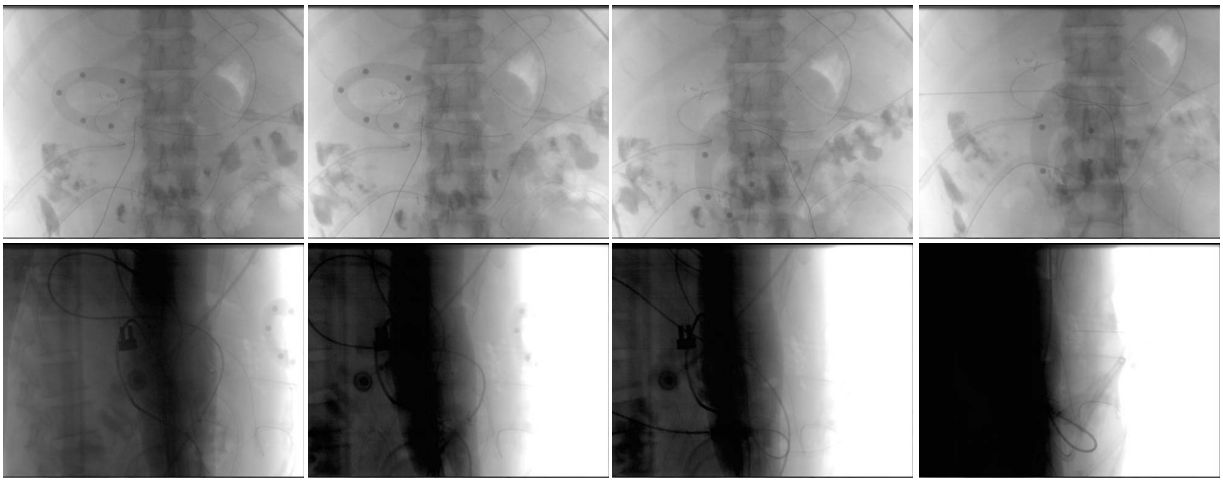

FIG. 5. Anterior-posterior (top) and lateral (bottom) views corresponding to the scans for the second patient in Table II.

tion after the third scan for patient 2. Figure 5 shows the AP and lateral views from the scans acquired for the second patient in Table II.

The above localization results confirm our assumption that in the clinical setting, fiducials that are located outside the reconstructed region will still be visible in a sufficient number of projection images for localization using our approach. Ideally, two images with perpendicular viewing directions will result in accurate localization. We have previously evaluated the effect of the number of images and their distribution on localization accuracy.[6] In that study, we observed that even two images with an angular difference of approximately 40° are sufficient to obtain submillimetric accuracy. Figure 6 illustrates the difference between localizing fiducials that are inside the reconstructed region and those that are not, as reflected by the projection images used to perform our localization.

Finally, we have also confirmed that in the clinical setting, the use of robust ray intersection is required; in our case, the use of the RANSAC framework successfully deals with these outliers. The outlying rays arise from erroneous fiducial localization in the projection images due to overlapping anatomical structures as shown in Fig. 7.

III.B. Quantitative evaluation

To evaluate the quality of localizations, we first compute the FRE for the direct localization approach and for our localization approach. As in both cases, each fiducial is localized separately: This quantity reflects the precision of each of the localization approaches. For direct localization, we obtained a mean (std) FRE of 0.13 (0.06) mm, and using our approach, the mean (std) FRE values are 0.29 (0.13) mm.

For the 28 fiducials that were inside the reconstructed region, we compute the distance between their 3D location as estimated with direct localization and that estimated using our approach. This quantifies the algorithm's accuracy, with direct localization serving as the gold standard. The mean (std) difference between the two localization approaches was 0.82 (0.34) mm. This error is our fiducial localization error (FLE).

Table III provides a more detailed view of our quantitative evaluation.

To assess if our localization approach is biased or not, we computed the mean (std) error per each of the X, Y, and Z coordinates. These errors are 0.15 (0.15), 0.37 (0.49), and −0.50 (0.38) mm, respectively. To assess the combined effect of the errors, we use the directional error. That is, we analyze the behavior of the normalized error vectors. If the error directions are uniformly distributed on the unit sphere, no directional bias, the norm of the mean vector is close to zero. If, on the other hand, the error directions are concentrated in a certain region, bias, the norm of the mean vector is closer to one.[10] In our case, the norm of the mean vector is 0.78. This indicates a bias which is visually discernable when overlaying the directional errors onto the unit sphere, as shown in Fig. 8.

Finally, while direct localization is currently the clinical gold standard, it is not necessarily more accurate than the proposed approach. As an example, we take the data set exhibiting the largest difference between the two approaches: Patient 2, scan 2. We projected the 3D locations estimated using both methods onto several x-ray images along the C-arm trajectory. From visual inspection, it appears that our approach is slightly more accurate than direct localization. Figure 9 shows a close up view of these images.

IV. DISCUSSION AND CONCLUSIONS

We have presented a patient databased evaluation of our method for spherical fiducial localization in C-arm based CBCT volumes directly from the projection images. The study included three patients undergoing navigated abscess drainage using a commercial navigation system. These cases clearly illustrated the challenge facing navigation systems if fiducial localization is performed directly in the reconstructed volume. Placing the fiducials on the patient's skin so

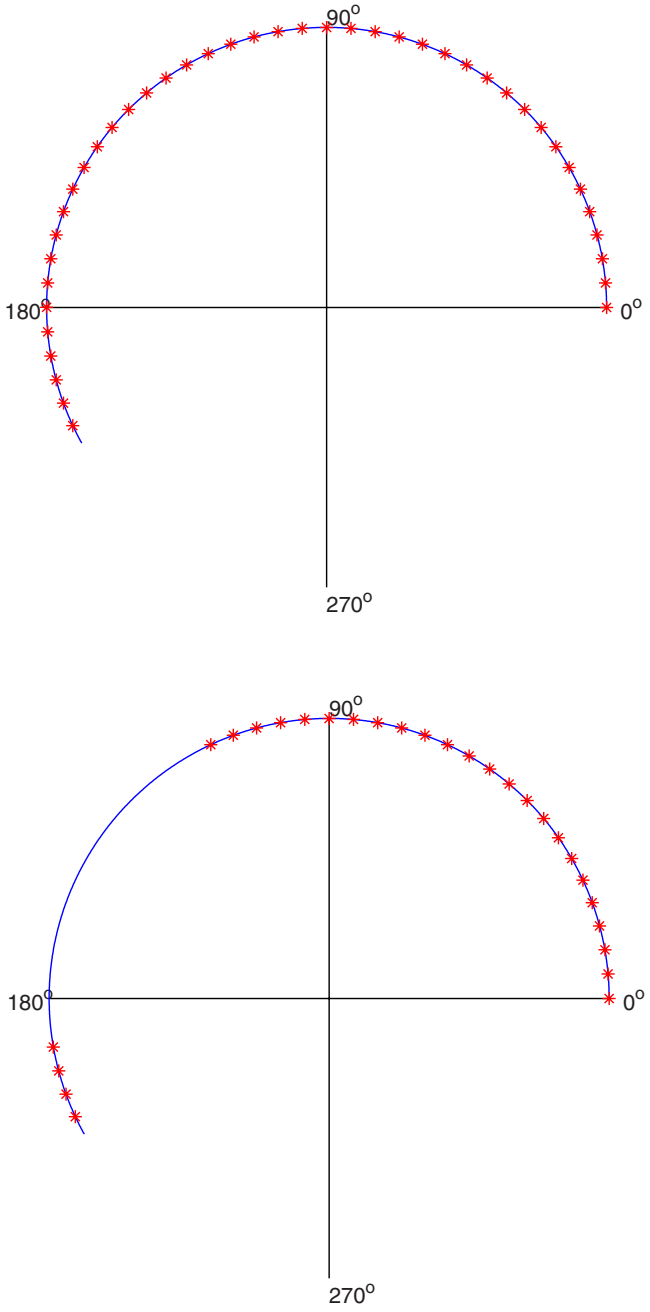

FIG. 6. Examples of image sets used for localization. C-arm orbit of 209°. On the top is the image set used for a fiducial contained in the reconstructed region (patient 2, scan 4) and on the bottom is an image set used for a fiducial found outside the reconstructed region (patient 2, scan 1). Images correspond to the use of our default sampling rate of every tenth image.

that both the fiducials and the anatomy of interest are inside the reconstructed region is not a trivial task. As a consequence, the patient may receive a higher radiation dose and the interventional workflow becomes more complex.

These two factors hinder the adoption of navigation systems for procedures utilizing C-arm based CBCT as the imaging modality. Concerns with regard to the patient's accumulated radiation exposure due to multiple CBCT acquisitions during a procedure have been previously raised.[11] It should also be noted that one of the goals of

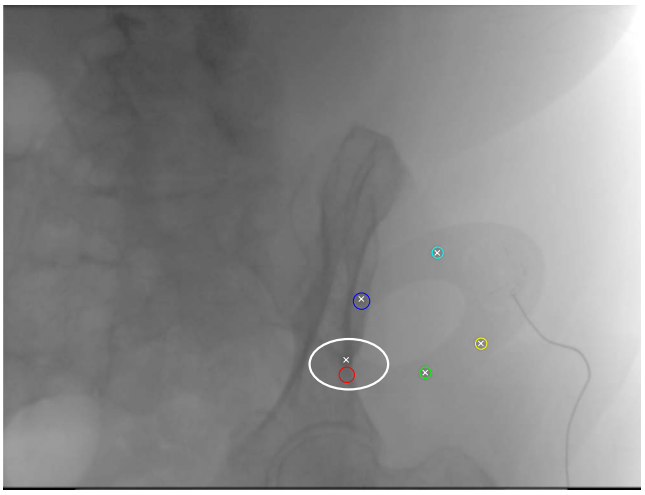

FIG. 7. Intersection of backprojected rays, 3D localization, is robust to outliers as it uses the RANSAC framework. Color (see electronic version) circles denote localized fiducials in the projection image and × denotes the projection of the localized fiducial in 3D back onto the x-ray image. The ellipse marks an outlying localization in 2D which is ignored during ray intersection as evident by the × projected onto the correct location.

navigation systems is to reduce the cumulative radiation exposure associated with frequent use of x-ray fluoroscopy, albeit primarily to the physician. In addition, the importance of a system's workflow on its adoption into clinical practice has been previously identified in Ref. 12. A complex workflow requiring changes to the fiducial placement and multiple volume acquisitions will reduce the chances of these systems being accepted into clinical practice.

Automated fiducial localization is desirable for a more streamlined clinical workflow. In our case, automatic, robust, and accurate fiducial localization is not trivial. This is primarily due to the variability in fiducial appearance. In the projection images, fiducials overlap different anatomical structures such as the ribs, the spinal column, or soft tissue. In addition, highly attenuating medical devices associated with patient treatment are also visible. Our semiautomatic ap-

TABLE III. Quantitative results summarizing the FRE associated with the two localization approaches and the distances between the two localizations. All values are in mm. Missing values occur for data sets in which all fiducials are outside the reconstructed region; in these cases, direct localization is not possible.

Data set		FRE from reconstruction	FRE from projection images	Mean (std) distance between localizations
Patient 1	1	⋯	0.10	⋯
	2	0.12	0.26	0.79 (0.08)
	3	0.16	0.19	0.66 (0.16)
Patient 2	1	⋯	0.24	⋯
	2	0.05	0.24	1.27(0.15)
	3	0.11	0.23	0.81 (0.39)
	4	0.09	0.40	0.93 (0.23)
Patient 3	1	⋯	0.35	⋯
	2	0.23	0.15	0.55 (0.42)

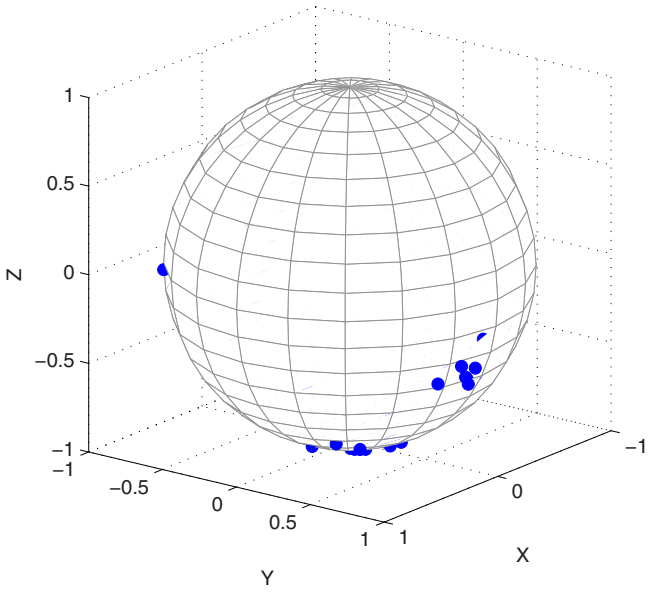

FIG. 8. Directional localization errors overlaid onto the unit sphere. A clear bias is visible.

proach provides robust and accurate fiducial localization by combining the human ability to easily recognize rough locations and the algorithm's ability to accurately localize fiducials given this manual initialization. As the approach only requires minimal interaction after image acquisition, its overall impact on procedure workflow is minor.

In this work we have shown that our proposed, x-ray projection, image based approach to fiducial localization is able to deal with clinical data, mitigating the inherent difficulties associated with direct fiducial localization. We have also observed that 2D erroneous fiducial localization does occur when fiducials overlap with osseous structures in the x-ray projection images. These outlying 2D localizations are later explicitly ignored via robust estimation of the backprojected rays' intersection.

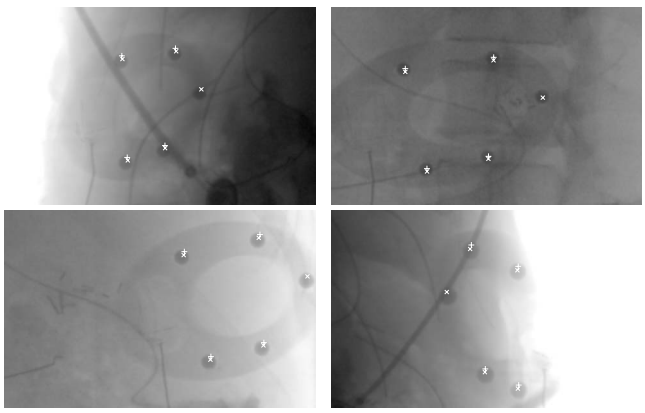

FIG. 9. Projection of 3D fiducial location onto x-ray frames acquired by CBCT (patient 2, data set 2). Frames correspond to C-arm angular poses of 24.5°, 74.5°, 124.5°, and 199.5°. + corresponds to direct fiducial localization and × corresponds to localization using our approach. The difference between our approach and direct fiducial localization in this case was between 1.1 and 1.4 mm. From visual inspection, our approach seems to provide better results than the direct localization, even though the FRE for that method is lower: 0.05 vs 0.24 mm.

To quantitatively evaluate our localization approach we used two quality measures, FRE, and the distance between fiducials localized using our approach and direct volumetric localization. From our results, we see that the direct approach is more stable with a mean (std) FRE of 0.13 (0.06) vs 0.29 (0.13) mm for our method. We use FRE to quantify the precision of each localization approach as each fiducial is localized independently from all others. Note that FRE does not reflect the accuracy of the localization as it is invariant under a rigid transformation. That is, any localization bias will be compensated for by the rigid transformation used in the computation of the FRE.

Assuming direct localization serves as ground truth, the mean (std) FLE is 0.82 (0.34) mm. This is slightly less accurate than our previous result of 0.51 (0.18) mm. Most likely, this is due to the coarser pixel spacing of the projection images acquired by the current clinical protocol 0.61×0.61 mm^2, which differs from the clinical protocol we had previously used (0.37×0.37 mm^2). Thus, the same subpixel localization accuracy will result in larger 3D localization differences. We have also found that the directional errors between the two approaches are biased. This is most likely due to the edge detection process used in the 2D localization. We use the Canny edge detector which applies Gaussian blurring prior to differentiation to suppress noise. On the one hand, use of a Gaussian with a larger standard deviation reduces the detector's sensitivity to noise. On the other hand, it increases the edge localization error. In our case, this is the most likely cause for a slight 2D fiducial localization bias, in turn leading to the exhibited 3D localization bias.

We note that a similar magnitude for FLE was observed in routine image-guided neurosurgical interventions.[13] In that context, a mean (std) FLE of 0.8 (0.6) mm was observed for localizing skin adhesive fiducials in MR volumes having a voxel size of $0.4 \times 0.4 \times 1$ mm^3. We thus conclude that our approach is sufficiently accurate for thoracic-abdominal interventions as these interventions generally require less accuracy than neurosurgical interventions.

Finally, while direct localization is the current standard of clinical practice, in some cases it seems that direct localization may be less accurate than our approach. This observation is based on visual inspection of the 3D data projected onto the x-ray images. It is thus unclear if direct localization should be viewed as a ground truth or only as the current clinically used localization method.

We have shown that using our localization approach in the clinic is possible and has the potential to reduce the cumulative radiation exposure to the patient, while at the same time simplifying the procedure's workflow, as compared to the standard direct volumetric localization. Using the proposed approach, the requirement that both the anatomy of interest and the skin fiducials be inside the reconstructed region is removed, making image-guided navigation systems utilizing C-arm based CBCT a viable clinical option.

ACKNOWLEDGMENTS

The authors thank Siemens AG Healthcare Sector for the loan of the iGuide CAPPA navigation system and Emmanuel Wilson for his help in obtaining the images used in this work.

[a]Electronic mail: zivy@isis.georgetown.edu

[1]D. Ritter, J. Orman, C. Schmidgunst, and R. Graumann, "3D soft tissue imaging with a mobile C-arm," Comput. Med. Imaging Graph. **31**, 91–102 (2007).

[2]M. J. Wallace *et al.*, "Three-dimensional C-arm cone-beam CT: Applications in the interventional suite," J. Vasc. Interv. Radiol. **19**, 799–813 (2008).

[3]K. Wiesent, K. Barth, N. Navab, P. Durlak, T. Brunner, O. Schütz, and W. Seissler, "Enhanced 3D-reconstruction algorithms for C-arm based interventional procedures," IEEE Trans. Med. Imaging **19**, 391–403 (2000).

[4]B. K. P. Horn, "Closed-form solution of absolute orientation using unit quaternions," J. Opt. Soc. Am. A **4**, 629–642 (1987).

[5]K. S. Arun, T. S. Huang, and S. D. Blostein, "Least-squares fitting of two 3-D point sets," IEEE Trans. Pattern Anal. Mach. Intell. **PAMI 9**, 698–700 (1987).

[6]Z. Yaniv, "Localizing spherical fiducials in C-arm based cone-beam CT," Med. Phys. **36**, 4957–4966 (2009).

[7]M. A. Fischler and R. C. Bolles, "Random sample consensus: A paradigm for model fitting with applications to image analysis and automated cartography," Commun. ACM **24**, 381–395 (1981).

[8]C. R. Maurer, Jr., J. M. Fitzpatrick, M. Y. Wang, R. L. Galloway, Jr., R. J. Maciunas, and G. S. Allen, "Registration of head volume images using implantable fiducial markers," IEEE Trans. Med. Imaging **16**, 447–462 (1997).

[9]J. M. Fitzpatrick, "Fiducial registration error and target registration error are uncorrelated," in Proceedings of SPIE Medical Imaging: Visualization, Image-Guided Procedures, and Modeling, 2009, Vol. 7261.

[10]J. P. Marques de Sá, *Applied Statistics Using SPSS, STATISTICA, MATLAB and R* (Springer, Berlin, 2007).

[11]R. C. Orth, M. J. Wallace, and M. D. Kuo, "C-arm cone-beam CT: General principles and technical considerations for use in interventional radiology," J. Vasc. Interv. Radiol. **19**, 814–820 (2008).

[12]Z. Yaniv and K. Cleary, "Image-guided procedures: A review," Technical Report No. CAIMR TR-2006-3 (Image Science and Information Systems Center, Georgetown University, 2006).

[13]R. R. Shamir, L. Joskowicz, S. Spektor, and Y. Shoshan, "Localization and registration accuracy in image guided neurosurgery: A clinical study," International Journal of Computer Assisted Radiology and Surgery **4**, 45–52 (2009).